J Fluoresc (2012) 22:1571–1579
DOI 10.1007/s10895-012-1097-2

ORIGINAL PAPER

The Application of CdTe/CdS in the Detection of Carcinoembryonic Antigen by Fluorescence Polarization Immunoassay

Jianniao Tian · Liujin Zhou · Yanchun Zhao · Yuan Wang · Yan Peng · Xue Hong · Shulin Zhao

Received: 10 February 2012 / Accepted: 20 June 2012 / Published online: 4 July 2012

Abstract A novel and portable strategy based on fluorescence polarization immunoassay (FPIA) using quantum dots (QDs) was described in this study for simple, rapid, and sensitive detection of carcinoembryonic antigen (CEA). Under optimal conditions, the sensor has a wide dynamic range (from 0.5 ng/mL to 200 ng/mL) and a good correlation. The limit of detection (LOD) is 0.21 ng/mL (S/N=3). The sensor has been applied for detection of carcinoembryonic antigen in 10 human serum samples with the range of recovery from 92.1 % to 103.6 %. Furthermore, bioconjugation of the core–shell QDs with streptavidin (SA) has been successfully applied in immunofluorescent imaging of the human hepatocellular carcinoma (HEPG2) cell line. The experimental results demonstrated the successful application of QDs-based fluorescence polarization immunoassay for detection of target proteins of biomedical importance. This strategy shows great promise for clinical diagnoses and basic discovery with high sensitivity, good specificity, simple procedures and short analysis time.

Keywords Fuorescence polarization immunoassay · Core–shell quantum dots · Carcinoembryonic antigen · Cell imaging

J. Tian (✉) · L. Zhou · Y. Zhao · Y. Wang · Y. Peng · X. Hong · S. Zhao
Key Laboratory for the Chemistry and Molecular Engineering of Medicinal Resources (Ministry of Education of China), College of Chemistry and Chemical Engineering of Guangxi Normal University,
Guilin 541004, China
e-mail: tianjn58@yahoo.com.cn

Y. Peng · X. Hong
College of Life Science, Guangxi Normal University,
Guilin 541004, China

Introduction

Carcinoembryonic antigen (CEA) [1], a kind of glycoprotein with a molecular mass of about 200 kDa found in colorectal carcinomas, is one of the most widely used tumor markers responsible for clinical diagnosis of colorectal, pancreatic, gastric, and cervical carcinomas [2, 3]. Thus, it either can be part of a panel of cancer markers for different cancers, more importantly; it also can be used as an independent prognostic factor. The normal CEA levels in healthy adults lie in the range 3–5 ng mL^{-1}, although some benign diseases can increase these levels up to 10 ng mL^{-1} [4–7]. When the CEA level is abnormally high before therapy, it is expected to fall to normal, following successful surgery or other treatment to remove the tumor. A rising CEA level indicates progression or recurrence of the cancer. In addition, levels of >20 ng mL^{-1} before therapy is commonly associated with cancer in the metastatic state [8, 9].

Several strategies have been developed for the detection of this important marker in the past such as enzyme-linked immunoassay [10], Raman Scattering based immunoassay [11], amperometric immunoassay [12, 13] and fluoroimmunoassay [14]. These systems all need to separate the free form and the complex of the antigen and the antibody, so that the accuracy and sensitivity of the assay are generally dependent on the quality of the separation, which is easily affected by sample composition. Moreover, enzyme-linked immunosorbent assay (ELISA) or other immunosorbent assay systems, in which antigen or antibodies are fixed on a solid surface, commonly associated with the decrease of protein bioactivity and the instability [10].

In the immunoassay method, fluorescence polarization immunoassay (FPIA) is the most extensively used homogeneous technique, which meets the requirements of a simple, reliable, fast and cost-effective analysis [15, 16]. FPIA method is based on the competition of free

(unlabeled) analyte and fluorescent-labeled antigen for antibody binding sites. Fluorescence emission is detected after excitation of the fluorescent probes with the plane-polarized light. The fluorescence polarization value is indirectly proportional to the analyte concentration as the analyte can bind to the high molecular weight species-like antibody [17]. It does not require a separation step to isolate antibody-bound label from unbound immunoreagent and is almost unique in this regard in small molecule (hapten) immunoassays [18].

The development of luminescent colloidal semiconductor nanocrystals referred to as quantum dots (QDs) [19] have led to an explosive growth in research on these materials. Compared to organic fluorophores, QDs exhibit more remarkable brightness, photostability, and excellent biological compatibility after appropriate surface-capping. Moreover, the high emission amplitude for QDs leads to a significant improvement in the signal to noise ratio of the final detected signals. These advantages make QDs attractive for the increased use of QDs as the fluorescent labels in immunoassays [20, 21]. Previous work has been done in our laboratory to develop a fluorescence polarization immunoassay for detection of alpha fetoprotein in human serum, the results indicates that QDs are attractive fluorescent probes in fluorescence polarization immunoassay [22].

In this study, we report a portable quantum dot-based fluorescence polarization immunoassay (FPIA) for simple, sensitive, and selective detection of carcinoembryonic antigen (CEA) in human serum. The approach developed in this work combines the advantage of the FPIA with the high sensitivity and the stability of quantum dot, which results in a novel, portable, and rapid competitive immunoassay tool for sensitive and selective detection of CEA.

Experimental

Materials

Thioglycolic acid (96 %), $NaBH_4$ (96 %), Tellurium powder (99.999 %) and $CdCl_2{\cdot}2.5H_2O$ (99 %), were obtained from Shanghai Chemical Reagents Company (China). 1-ethyl-3(3-dimethy laminopropyl) carbodiimide hydrochloride (EDC) and N-hydroxysuccinimide (NHS) were purchased from Sigma-Aldrich. Mouse anti-Rbbit IgG/biotin and streptavidin (SA) were obtained from Beijing Biosynthesis Biotechnology Co. (China). Monoclonal anti-CEA and CEA(98 %) were purchased from Shuangliu Zhenglong Laboratory of Biochemical Products (Chengdu, China). All other reagents were of analytical reagent grade and used without further purification. Ultrapure water with 18.2 MΩ cm^{-1} was used in our experiments.

Synthesis of CdTe QDs, CdTe/CdS QDs

Highly fluorescent CdTe QDs nanocrystals were made by a procedure modified as reported [23]. Then the purify CdTe core QDs were injected into the Cd^{2+}–TGA precursor solution ($[Cd^{2+}]/[TGA]=1$, pH=9.00). The CdTe/CdS precursor solution was put into a flask, and heated to 80 °C in argon atmosphere and the thioacetamide (TAA) solution was injected into the flask with continuous stirring. The CdTe/CdS core–shell QDs(photoluminescence quantum yields (PLQY)≈60 %, determined by the comparative method [24]) were obtained after different refluxing times. All of the nanocrystals were purified by acetone precipitation and then dissolved in phosphate-buffered saline (PBS).

Preparation of Streptavidin-Conjugated QDs and CEA Conjugation

The mixture EDC (5 μL, 0.056 M) and sulfo-NHS (5 μL, 0.1 M) were added to the QDs in PBS (pH 7.40) solution and activated for 15 min. Activated QDs were mixed with 10 μg mL^{-1} streptavidin (SA) and reacted for 4 h at room temperature, the SA-conjugated QDs were separated from the solution by an ultracentrifuge filter (MWCO=50 000 Da). The resulting solution was then stored at 4 °C in the dark for future use.

In addition, 8.4 μg CEA was added to the activated CdTe/CdS QDs solution and kept at room temperature for 2–3 h. After reaction at 4 °C overnight, an ultracentrifuge filter (MWCO=50 000 Da) was employed to purify the CEA-QDs.

Characterization of Streptavidin- QDs and CEA-QDs

For size-exclusion high-performance liquid chromatography (HPLC), the mobile phase was 0.5 M PBS (pH 7.40), at a flow rate of 0.5 mL min^{-1}. The protein PAK 125 column (7.8 mm×30 cm) was washed with PBS for 2 h, and then 15 μL samples were injected into gel separation column. The major peaks were detected by waters 2487 UV detector (Waters, USA) at 280 nm. Photoluminescence (PL) measurements were performed at room temperature using a LS-55 luminescence spectrometer (Perkin Elmer, USA) with the excitation wavelength 370 nm. Fluorescence emission spectra were collected at 480–680 nm range. The slit widths for both monochromators were fixed at 8 nm.

Cell Imaging

As showed in Fig. 1, the human hepatocellular carcinoma cells HepG2.2.15 were cultured on a circular cover slip in Dulbecco's Modified Eagle's Medium (DMEM) with 10 % (v/v) fetal bovine serum (FBS) overnight. The HepG2.2.15 cells were fixed with 4 % paraformaldehyde for 15 min, then

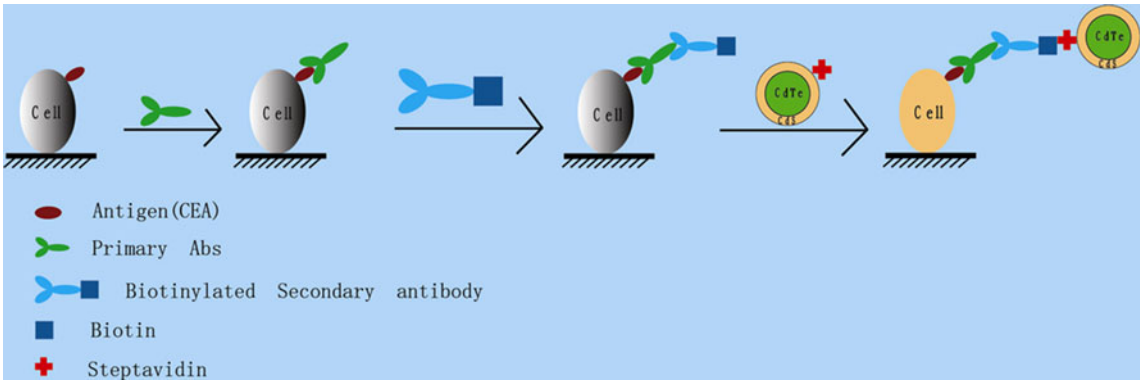

Fig. 1 Schematic diagram of microscopic images of the cells

washed with PBS three times, and blocked with 1 % bovine serum albumin (BSA) in PBS for 2 h before loading the primary antibody. The monoclonal anti-CEA was diluted in PBS (1:200), and 100 μL of the diluted monoclonal antibody was added to each cover slip for further incubation at 4 °C overnight. After washing the cover slips with PBS three times for 5 min, 100 μL of mouse anti-rabbit IgG antibody conjugated with biotin (1:200 dilution in PBS) was loaded onto each cover slip and incubated at room temperature for 2 h. The cover slips were washed with PBS three times for 5 min and incubated in SA-CdTe/CdS QDs at room temperature for 1 h. Then the cover slips were washed and were imaged at room temperature. The fluorescence images of cells were obtained with a Nikon inverted microscope (Nikon TE2000-S, Japan) which was equipped with a high-definition CCD camera, a 100 W Hg excitation lamp and three filters (λ_{ex} 350±20 nm, λ_{ex} 470±20 nm and λ_{ex} 535±20 nm).

Fluorescence Polarization Immunoassay

Figure 2 shows the schematic diagram of the Fluorescence polarization immunoassay procedure. Specific steps as follows: 700 μL of CEA standard solutions, 700 μL of purify CEA-QD solution and 700 μL of the optimal dilution of anti-CEA were added into a cuvette. The reaction mixture was vortex-mixed, allowed to stand for 5 min, and then measured in the fluorescence spectrophotometer. Serum samples were carried out on a 50 000 MW size filter and centrifugation at 3000g for 15 min at 4 °C to remove low molecular weight protein (<50 000 Da). The upper phase was decanted, dissolved in PBS and subjected additionally.

All experiments were carried out at 25 °C. The fluorescence polarization immunoassay was performed on an automated polarization model FL3-P-TCSPC(HORIBA JOBIN YVON, France). The fluorescence intensity and fluorescence polarization of the immunocomplex were monitored by exciting the sample at 370 nm and measuring the emission at 580 nm. Fluorescence polarization was measured using the L-format configuration, using FluorEssence™ software such as constant wavelength analysis to achieve a polarization value. The polarization value was also calculated automatically by the instrument. The integration time was set to 3 s for the polarization measurements. Over six polarization measurements were taken each time, and they were then averaged for further data processing. The relative standard deviation was 2 % for all measurements.

Results and Discussion

Synthesis and Biophysical Characterization of CEA-QDs

An excess amount of CEA was allowed to react with activated amino CdTe/CdS QDs 580. The formation of QDs bioconjugates was confirmed by HPLC size exclusion chromatography (Fig. 3). Since the species with higher

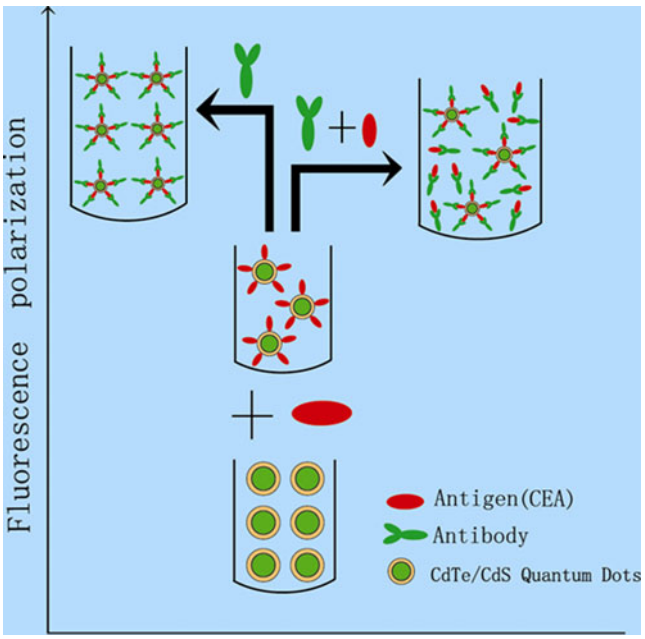

Fig. 2 Schematic diagram of the Fluorescence polarization immunoassay

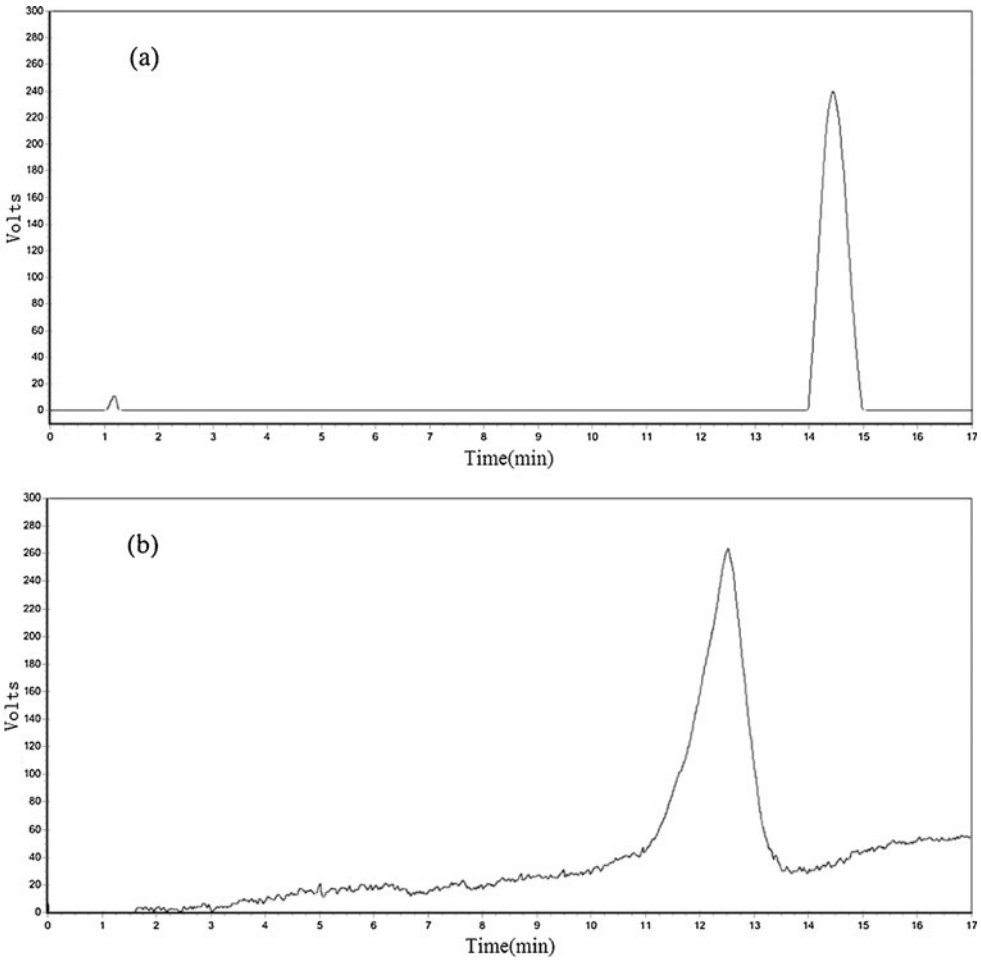

Fig. 3 HPLC elution curves for **a** free CEA and **b** QDs580-CEA. The retention times of free CEA and QDs580-CEA were about 14.48 min and 12.24 min, respectively. The mobile phase was 0.5 M PBS (pH 7.4), and the flow rate was 0.5 mL min^{-1}

molecular weights are eluted in shorter retention times, the observed HPLC peaks at a retention time 14.48 min were attributed to free CEA (Fig. 3a). After the conjugation to CdTe/CdS QDs, the peaks can be seen at 12.24 min, which was considered the signal of higher molecular weight, as expected for the attachment of QDs to CEA (Fig. 3b).

To evaluate whether there was any difference in the photoluminescence (PL) spectrum of CdTe/CdS QDs 580 after conjugation to CEA, PL measurements of CdTe/CdS QDs 580 were performed by excitation with a 370 nm laser. From Fig. 4, water soluble CdTe/CdS quantum dots synthesized by us have good fluorescence properties of strong fluorescence and desirable symmetry of peak. Furthermore, the spectrum of CEA-CdTe/CdS QDs 580 is still symmetrical and almost identical to that of QDs with only a slight red shift. The results demonstrated that the optical properties of the CdTe/CdS QDs 580 were not altered after functionalization with the CEA.

Antibody Dilution Curve and CEA-QDs Concentration for Fluorescence Polarization Immunoassay

As reptorted, the lower QDs580-labeled antigen concentration, which has no effect on the fluorescence signal, the lower sensitivity will be obtained. In previous studies, the lowest QDs580-labeled antigen concentration giving a signal should be approximately 10 times higher than the background signal from PBS (total fluorescence intensity) [17]. So, here, the amount of CEA-QDs580 was selected such that the total final fluorescence intensity was 10 times higher

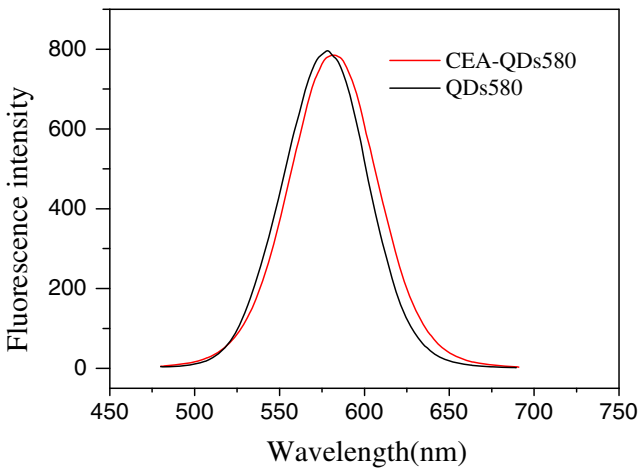

Fig. 4 Fluorescence emission spectra of QDs580 and CEA-QDs580. *c* (QDs580)=25 μM; 0.5 M PBS (pH 7.4); 25 °C.

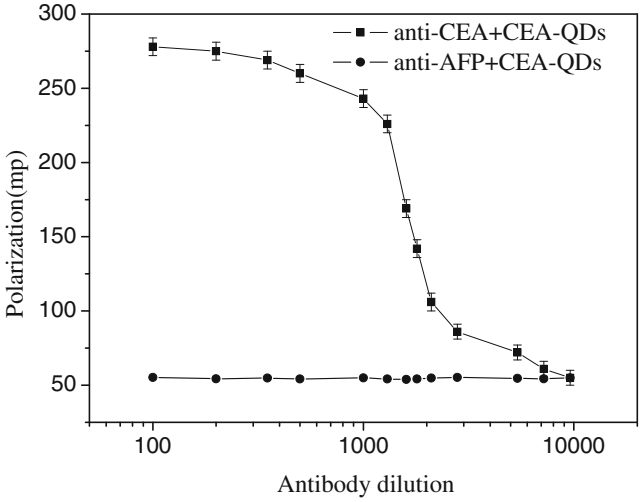

Fig. 5 Dilution curves for anti-CEA and nonspecific anti-AFP

than the background of PBS, and the concentration of CEA-QDs580 was1.25×10^{-6} mol·L^{-1}.

The anti-CEA was serially diluted 1/100, 1/200……1/9600 in PBS. Then 1 mL of diluted antibody solution was added to 1 mL of fixed amounts QDs580-labeled antigen in PBS. The reaction mixture was vortex-mixed, allowed to stand for 5 min, and then measured in the fluorescence spectrophotometer. The obtained results are presented as the curves with fluorescence polarization units plotted against antibody dilutions, as showed in Fig. 5. Fluorescence polarization values resulting from QDs580-labeled antigen binding with specific monoclonal anti-CEA antibodies and with nonspecific anti-AFP were compared. It can be seen in Fig. 5 that the specific monoclonal anti-CEA antibodies gave significant binding with QDs580-labeled antigen at higher concentration and slowly decreased in FP as anti-CEA antibodies became more diluted by PBS. However, the QDs580-labeled antigen always had similar FP values in spite of the change of nonspecific anti-AFP concentration. The results indicate that the QDs580-labeled antigen was successfully synthesized and could be used as a competition agent in the FPIA. The dilution of antibody corresponding to 50 % QDs580-labeled antigen binding was chosen as the titer value because this dilution may be optimal for FPIA standard curves [25, 26]. As showed in Fig. 5 the dilution of antibody was 1/1800.

The Standard Curve for CEA Determination in Fluorescence Polarization Immunoassay

Microcal Origin software was employed to plot and calculate the analytical parameters of the immunoassays [IC_{50} values, slope, and standard deviations (SD)]. The standard curve for CEA determination was plotted as relative current values. The analyte concentrations and the polarization signal were fitted to a sigmoid curve according to the formula: $Y = (A_1 - A_2)/[1 + (\frac{X}{X_0})^P] + A_2$, where A_1 and A_2 are the maximal and minimal polarization signals, P is the slope of the sigmoid curve, and X_0 expressed as IC_{50} value [17, 27].

As shown in Fig. 6, in the fixed concentration of anti-CEA solution, labeled and unlabeled CEA is allowed to simultaneously compete for the binding sites on the anti-CEA. The concentration of labeled CEA was fixed, and the concentration of unlabeled CEA was changed. When unlabeled CEA antigen was added, the polarization signals were obviously weaken with the increase in its concentration. The values of A_1 and A_2 were 137.68, 52.26 respectively, and

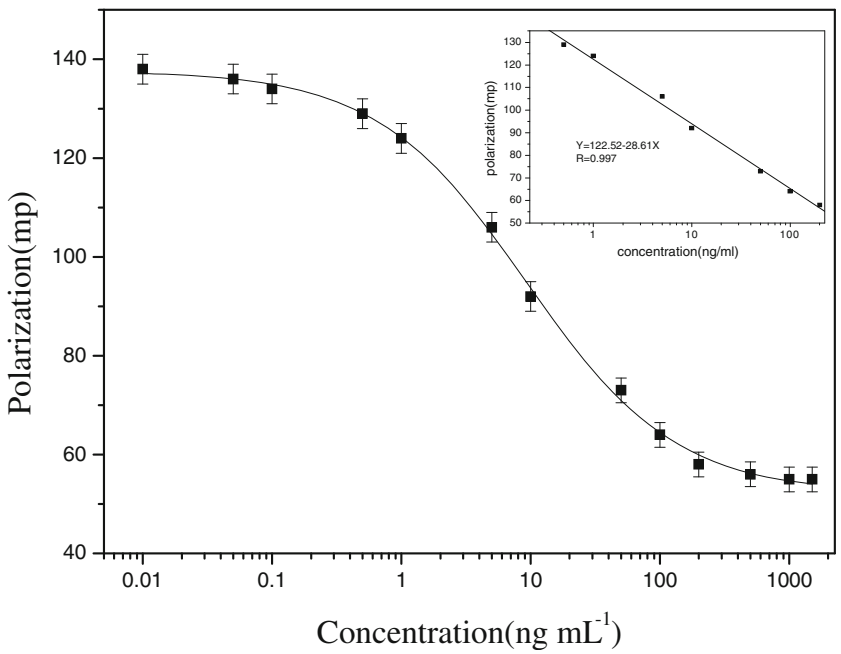

Fig. 6 FPIA calibration curves for CEA

the X_0 was 9.24 ng mL^{-1}, R^2=0.999. The concentration of unlabeled CEA was varied from 0.01 ng mL^{-1} to 1.5 μg mL^{-1}. The linear range of unlabeled CEA concentrations at calibration curves corresponds to the range from 0.5 ng mL^{-1} to 200 ng mL^{-1} with correlation coefficient 0.997. The limit of detection (LOD), which was determined from calibration curve using the blank signal (that is defined as an average from five mesurements of zero analyte dose signal) and the three-fold confidence interval [28], was 0.21 ng ml^{-1}. Each measurement for date points was repeated about six times.

Detection of Serum CEA Levels

The serum CEA levels in five normal human serum samples and five carcinoma patient's serum samples were detected by using the proposed QD580 immunosensor. For analyses of practical samples, the interference and fluorescence quenching by some serum samples should be taken into account [22]. In this paper, the advanced process of centrifugation with an ultracentrifuge filter was performed to remove unrelated protein in the serum. As showed in Table 1, the mean serum CEA concentrations obtained by the proposed CEA immunosensor were agree with the reference values, which were measured by the standard ELISA [29]. The relative errors of the results acquired by these methods were less than 3.5 %. The recovery for CEA was from 92.1 to 103.6 % showed in Table 2. Therefore, the fluorescence polarization immunoassay could be satisfactorily applied to the clinical determination of the CEA level in humans.

Cell Images

To determine the advantage of QDs580 in biomedical application, we attempted the detection of CEA on the surface of some hepatocellular cancer cells. As showed in Fig. 7, 7702 (human liver cells, CEA negative), and HepG2 (human hepatocellular carcinoma cells, high CEA expression) cells were blocked with 0.1 % bovine serum albumin, stained with 1 nM QD580-SA in the presence of Mouse anti-Rbbit IgG antibody conjugated with biotin (1:200 dilution in PBS) and examined under the microscope. The representative bright field and fluorescence images are shown in Fig. 7.

It can be seen clearly that QD580-SA did not bind to CEA-negative cells (7702, f), because there is a minimal fluorescence signal observed, whereas the CEA-positive cells (HepG2, b, d) are clearly visualized. Moreover, control studies using QD-SA (without antibody) showed nonspecific binding to HepG2 (Fig. 7d), which bright fluorescence signal can be seen in the whole nucleus of cells. Besides, in the design of the immunofluorescent imaging of cells (Fig. 7b), the bright fluorescence of QDs mainly appears in the cytoplasm of the cell. There are many ways of intracellular delivery of QDs for live cell labeling and organelle tracking [30], such as biochemical methods (translocation peptides, cationic liposomes, dendrimers) and physical methods (electroporation and microinjection) [31]. Generally speaking, there are two kinds of mechanisms including non-specific entry by endocytosis [32] and specific entry mediated by biomolecules attached to QD surface [33–35]. The process for the QD-SA to enter HepG2 cells might be endocytosis, where streptavidin can facilitate the delivery of QDs into HepG2 cells, but it is difficult for intact 7702 cells. For immunofluorescent imaging of HepG2 cells, the streptavidin–biotin binding scheme was employed to conjugate antibodies to the SA-coated core-shell QDs because of their strong noncovalent affinities. One streptavidin molecule can combine with four biotin molecules, which induces the magnification of signals [36]. It can be seen that the bright fluorescence of QDs mainly appears in the cytoplasm of the cell. This indicates that the SA-QD is mainly integrated with the CEA in the cytoplasm, which is in agreement with the theory that CEA is expressed in the cytoplasm of tumor cells [1, 37]. These results established that the anti-CEA–QD conjugates retain their CEA binding activity and specificity.

Table 1 Detection of CEA in human serum

Sample	Content (ng mL^{-1})	Mean value (ng mL^{-1})	RSD(%)	Reference value (ng mL^{-1})
1	2.19, 2.13, 2.19, 2.05, 2.24	2.16	3.32	2.25
2	2.72, 2.65, 2.63, 2.59, 2.63	2.64	2.02	3.08
3	4.73, 4.70, 4.77, 4.62, 4.89	4.74	2.09	4.56
4	5.43, 5.39, 5.43, 5.56,5.30	5.42	1.75	5.21
5	1.55, 1.56, 1.52, 1.49,1.51	1.52	1.92	1.78
6	23.87, 23.68, 23.49, 24.26, 22.93	23.68	2.08	23.32
7	117.46,116.52,117.46, 19.37, 114.66	117.10	1.46	117.26
8	191.92,188.85,193.47, 88.85, 187.34	190.09	1.33	189.78
9	100.0,101.62,101.62, 98.40, 99.20	100.17	1.44	101.35
10	134.69,135.78,133.61, 132.54, 132.54	133.83	1.05	132.87

1–5 samples come from healthy adults' serum, 6–10 samples come from lung cancer, uterine cancer, hepatic carcino.ma, breast cancer and gastric cancer patient, respectively

Table 2 The recovery of CEA in human serum samples

Sample	Content (ng mL^{-1})	Added (ng mL^{-1})	Found (ng mL^{-1})	Recovery (%)
1	2.16	5	6.59	92.1
2	2.64	5	7.52	98.4
3	4.74	5	9.92	101.8
4	5.42	5	10.31	98.9
5	1.52	5	6.27	96.2
6	23.68	50	73.46	99.7
7	117.10	50	173.12	103.6
8	190.19	50	228.9	95.3
9	100.17	50	147.77	98.4
10	133.83	50	182.36	99.2

Conclusions

In summary, QDs as a promising alternative reporter has been successfully integrated with FPIA and developed for rapid, sensitive, and one-step quantitative detection of carcinoembryonic antigen. This approach takes advantage of high sensitivity and easy procedures of fluorescence polarization immunoassay and photostability of QDs. Under optimal conditions, this proposed QDs-based FPIA have a linear relationship in the range of 0.5 ng mL^{-1} to 200 ng mL^{-1} with a detection limit of 0.21 ng mL^{-1}. Furthermore, the cell images indicate that the SA-coated core-shell QDs have a very good signal in a biotin–streptavidin labeling system. Overall, the QDs-based FPIA, considered as an advance in alternative immunoassay, has a great potential for rapid, sensitive, and simple analysis of other protein biomarkers in clinical diagnostics, basic discovery, and a variety of other biomedical applications.

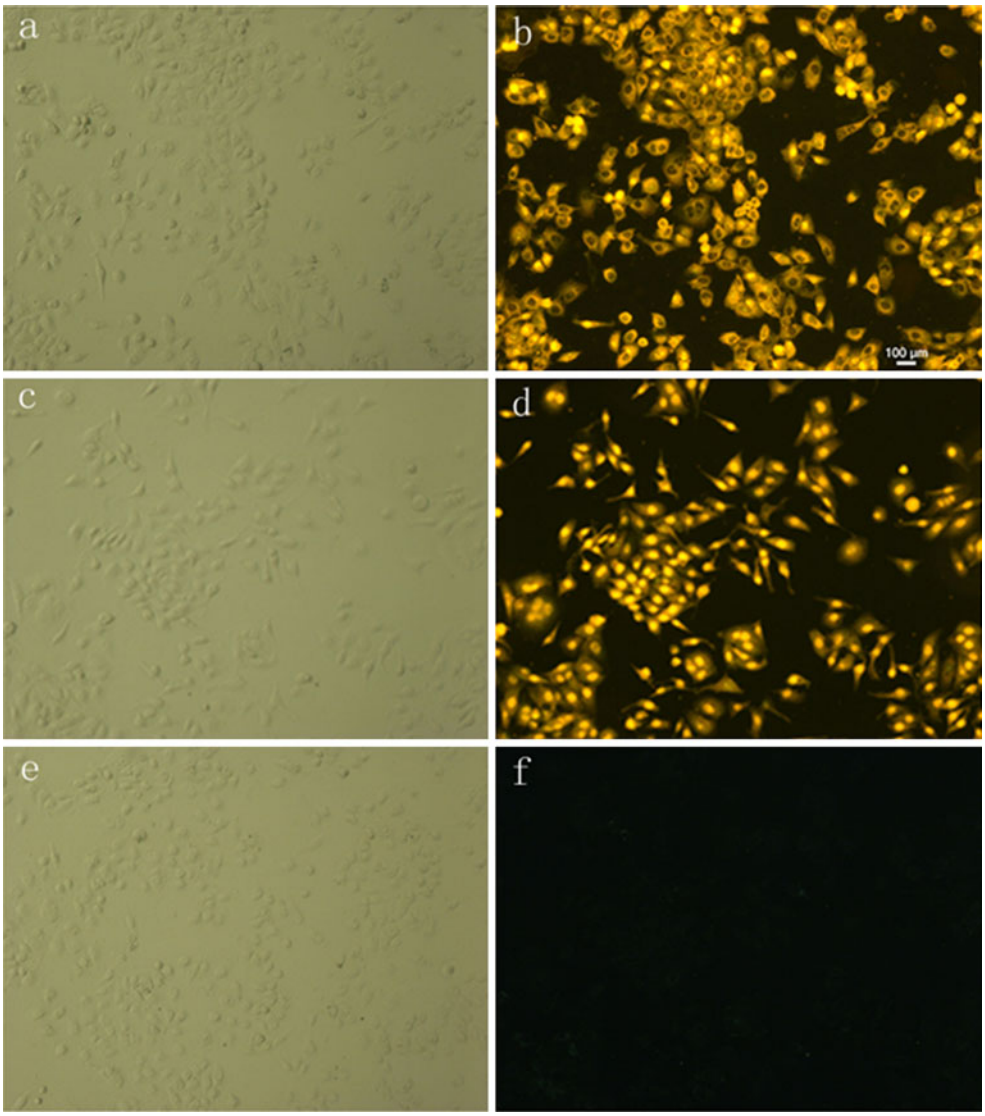

Fig. 7 Microscopic images of the cells. **a**, **b** HePG2 cells, which are CEA-positive, as revealed by the presence of the anti-CEA-Bio-SA-QDs 580 Ab bioconjugate on the cell surface. **c**, **d** Negative staining was detected in HePG2 cells exposed to SA-QDs580 in the absence of anti-CEA. **e**, **f** Negative staining in 7702 cells that lack CEA expression by the presence of the anti-CEA-Bio-SA-QDs580 Ab bioconjugate on the cell surface as a control. **a**, **c**, **e** bright field; **b**, **d**, **f** fluorescence. All fluorescence images were recorded at 20x magnification using a Nikon inverted microscope (Nikon TE2000- S, Japan) which was equipped with a high-definition CCD camera, a 100 W Hg excitation lamp and three filters (λex 350±20 nm, λex 470± 20 nm and λex 535±20 nm)

Acknowledgements This work has been supported by National Natural Science Foundation of China (No. 21165004, 21163002), the Guangxi Natural Science Foundation of China (2010GXNSFF013001, 0728043), Innovation Plan in Graduate Education of Guangxi Province (2010106020703M70) and the project of Key Laboratory for the Chemistry and Molecular Engineering of Medicinal Resources(Guangxi Normal University), Ministry of Education of China(CMEMR2011-14).

References

1. Gold P, Shuster J, Freedman SO (1978) Carcinoembryonic antigen (CEA) in clinicalmedicime. Cancer 42:1399–1405
2. Goldenberg DM, Sharkey RM, Primus FJ (1976) Carcinoembryonic antigen in hist opathology: immunoperoxidase staining of conventional tissue sections. Natl Cancer Inst 57:11–22
3. Tang DP, Yuan R, Chai YQ (2006) Magnetic core shell Fe_3O_4@Ag nanoparticles coated carbon paste interface for studies of carcinoembryonic antigen in clinical immunoassay. J Phys Chem B 110:11640–11646
4. Laboria N, Fragoso A, Kemmner W, Latta D, Nilsson O, Botero ML, Drese K, O'Sullivan CK (2010) Amperometric immunosensor for carcinoembryonic antigen in colon cancer samples based on monolayers of dendritic bipodal scaffolds. Anal Chem 82:1712–1719
5. Molina R, Judith J, Filella X, Zanon G, Pahisa J, Munoz M, Farrus B, Latre ML, Escrichc C, Estape J, Ballesta AM (1998) C-erbB-2 oncoprotein, CEA, and CA15.3 in patients with breast cancer: prognostic value. Breast Cancer Res Treat 51:109–119
6. Mujagic Z, Mujagic H, Prnjavorac B (2004) The relationship between circulating carcinoembryonic antigen (CEA) levels and parameters of primary tumor and metastases in breast cancer patients. Med Arh 58:23–26
7. Theriault RL, Hortobagyi GN, Fritsche HA, Frye D, Martinez R, Buzdar AU (1989) The role of serum CEA as a prognostic indicator in stage II and III breast cancer patients treated with adjuvant chemotherapy. Cancer 63:828–835
8. Macdonald JS (1999) Carcinoembryonic antigen screening: pros and cons. Semin Oncol 26:556–560
9. Dnistrian AM, Schwartz MK, Greenberg EJ, Smith CA, Schwartz DC (1991) CA15-3 and carcinoembryonic antigen in the clinical evaluation of breast cancer. Clin Chim Acta 200:81
10. Yang HJ, Jiang SJ, Yang YJ, Hwang CJ (1995) Speciation of tin by reversed phase liquid chromatography with inductively coupled plasma mass spectrometric detection. Anal Chim Acta 312:141–148
11. Chon H, Lee S, Son SW, Oh CH, Choo J (2009) Highly sensitive immunoassay of lung cancer marker carcinoembryonic antigen using surface-enhanced raman scattering of hollow gold nanospheres. Anal Chem 81:3029–3034
12. Tang DP, Ren JJ (2008) In situ amplified electrochemical immunoassay for carcinoembryonic antigen using horseradish peroxidase-encapsulated nanogold hollow microspheres as labels. Anal Chem 80:8064–8070
13. Shiku H, Matsue T, Uchida I (1996) Detection of microspotted carcinoembryonic antigen on a glass substrate by scanning electrochemical microscopy. Anal Chem 68:1276–1278
14. Yuan JL, Wang GL, Majima K, Matsumoto K (2001) Synthesis of a terbium fluorescent chelate and its application to time-resolved fluoroimmunoassay. Anal Chem 73:1869–1876
15. Shim WB, Kolosova AY, Kim YJ, Yang ZY, Park SJ, Eremin SA, Lee IS, Chung DH (2004) Fluorescence polarization immunoassay based on a monoclonal antibody for the detection of ochratoxin A. Int J Food Sci Tech 39:829–837
16. Latychevskaiab TY, Renna A, Wild UP (2006) A single-molecule study of polycrystalline microstructure by fluorescence polarization spectroscopy. J Lum 118:111–122
17. Eremin SA, Murtazina NR, Ermolenko DN, Zherdev AV, Mart'ianov AA, Yazynina EV, Michura IV, Formanovsky AA, Dzantiev BB (2005) Production of polyclonal antibodies and development of fluorescence polarization immunoassay for sulfanilamide. Anal Lett 38:951–969
18. Murtazina NR, Eremin SA, Mozoleva OV, Everest SJ, Brown AJ, Jackman R (2004) Fluorescent polarization immunoassay for sulphadiazine using a high specificity antibody. Int J Food Sci Tech 39:879–889
19. Gao XH, Cui YY, Levenson RM, Chung LWK, Nie SM (2004) In vivo cancer targeting and imaging with semiconductor quantum dots. Nat Biotech 22:969–976
20. Chen W, Peng CF, Jin ZY, Qiao RR, Wang WY, Zhu SF, Wang LB, Jing QH, Xu CL (2009) Ultrasensitive immunoassay of 7-aminoclonazepam in human urine based on CdTe nanoparticle bioconjugations by fabricated microfluidic chip. Biosens Bioelectron 16:2051–2056
21. Warner MG, Grate JW, Tyler A, Ozanich RM, Miller KD, Lou JL, Marks JD, Bruckner-Le CJ (2009) Quantum dot immunoassays in renewable surface column and 96-well plate formats for the fluorescence detection of botulinum neurotoxin using high-affinity antibodies. Biosens Bioelectron 25:179–184
22. Tian JN, Liu RJ, Zhao YC, Peng Y, Hong X, Xu Q, Zhao SL (2010) Synthesis of CdTe/CdS/ZnS quantum dots and their application in imaging of hepatocellular carcinoma cells and immunoassay for alpha fetoprotein. Nanotechnology 21: 305101–305108
23. Tian JN, Liu RJ, Zhao YC, Xu Q, Zhao SL (2009) Controllable synthesis and cell-imaging studies on CdTe quantum dots together capped by glutathione and thioglycolic acid. J Colloid Interf Sci 336:504–509
24. Fery-Forgue S, Lavabre D (1999) Are fluorescence quantum yields to tricky to measure? A demonstration using familiar stationary products. J Chem Ed 76:1260–1264
25. Önnerfjord P, Eremin S, Emnéus J, Marko-Varga G (1998) Fluorescence polarisation for immunoreagent characterization. J Immunol Methods 213:31–39
26. Zhan HW, Lin LC, Wei MS, Su XZ, Jian ZS (2010) Fluorescence polarization immunoassay for salinomycin based on monoclonal antibodies. Sci Chin Chem 53:553–555
27. Ekins R, Edwards P (1997) On the meaning of 'sensitivity'. Clin Chem 43:1824–1837
28. Pourfarzaneh M, White GW, Landon J, Smith DS (1980) Cortisol directly determined in serum by fluoroimmunoassay with magnetizable solid phase. Clin Chem 26:730–733
29. Niculescu F, Rus HG, Ionescu D, Maican A, Petcovici M, Malide D, Rahaian R (1989) Isolation of anti-carcinoembryonic antigen (CEA), specific immunoglobulins and their use in immunecytochemical and enzyme-immunoassays(ELISA). Arch Roum Pathol Exp Microbiol 72:47–52
30. Derfus AM, Chan WCW, Bhatia SN (2004) Intracellular delivery of quantum dots for live cell labeling and organelle tracking. Adv Mat 16:961–966
31. Xie MX, Liu HH, Chen P, Zhang ZL, Wang XH, Xie ZX, Du YM, Pan BQ, Pang DW (2005) CdSe/ZnS-labeled carboxymethyl chitosan as a bioprobe for live cell imaging. Chem Commun 5518–5520
32. Jaiswal JK, Mattoussi H, Mauro JM, Simon SM (2003) Long-term multiple color imaging of live cells using quantum dot bioconjugates. Nat Biotechnol 21:47–51
33. Voura EB, Jaiswal JK, Mattoussi H, Simon SM (2004) Tracking metastatic tumor cell extravasation with quantum dot nanocrystals and fluorescence emission-scanning microscopy. Nat Med 10:993–998
34. Chan WC, Nie SM (1998) Quantum dot bioconjugates for ultrasensitive nonisotopic detection. Science 281:2016–2018

35. Chen FQ, Gerion D (2004) Fluorescent CdSe/ZnS nanocrystal-peptide conjugates for long-term, nontoxic imaging and nuclear targeting in living cells. Nano Lett 4:1827–1832
36. Haiqiang Y, Edwin L, Stephen WY, Jian L, Hui T, Ping C (2006) Quantitative analysis of free fatty acids in rat plasma using matrix-assisted laser desorption/ionization time-of-Xight mass spectrometry with meso-tetrakis porphyrin as matrix. Anal Biochem 354:182–191
37. Chen G, Desen W, Hou JH, Lin SX, Pan ZZ, Zhou ZW, Chen YB (2001) Tissue CEA and its clinicobiologieal significance in patients with colorectral cancer. Chin J Cancer 20:628–630